

AlGaInP laser diodes incorporating a 3λ/4 multiple quantum barrier

A. Sobiesierski, I. C. Sandall, P. M. Smowton, P. Blood, A. B. Krysa et al.

Citation: *Appl. Phys. Lett.* **86**, 021102 (2005); doi: 10.1063/1.1849847

View online: <http://dx.doi.org/10.1063/1.1849847>

View Table of Contents: <http://apl.aip.org/resource/1/APPLAB/v86/i2>

Published by the [American Institute of Physics](#).

Additional information on *Appl. Phys. Lett.*

Journal Homepage: <http://apl.aip.org/>

Journal Information: http://apl.aip.org/about/about_the_journal

Top downloads: http://apl.aip.org/features/most_downloaded

Information for Authors: <http://apl.aip.org/authors>

ADVERTISEMENT



ACCELERATE AMBER AND NAMD BY 5X.
TRY IT ON A FREE, REMOTELY-HOSTED CLUSTER.

LEARN MORE

AlGaInP laser diodes incorporating a $3\lambda/4$ multiple quantum barrier

A. Sobiesierski, I. C. Sandall, P. M. Smowton,^{a)} and P. Blood
School of Physics and Astronomy, Cardiff University, Cardiff CF24 3YB, United Kingdom

A. B. Krysa
EPSRC National Centre for III-V Technologies, Department of Electronic and Electrical Engineering, University of Sheffield, Mappin Street, Sheffield S1 3JD, United Kingdom

M. R. Brown, K. S. Teng, and S. P. Wilks
Multidisciplinary Nanotechnology Centre, School of Engineering, University of Wales Swansea, Singleton Park, Swansea SA2 8PP, United Kingdom

(Received 31 August 2004; accepted 22 November 2004; published online 30 December 2004)

Using segmented contact measurements to determine gain versus quasi-Fermi level separation and nonradiative recombination we demonstrate that placing a multiquantum barrier (MQB) within the *p*-type cladding of 670 nm AlGaInP laser diodes reduces electron leakage current as a function of quasi-Fermi level separation compared to otherwise identical reference devices. At 300 K, where thermally activated leakage is absent, devices with and without a MQB have the same threshold current density whereas at 375 K the threshold current density of a 320 μm laser is reduced by $1735 \pm 113 \text{ A cm}^{-2}$ for the device containing the MQB. © 2005 American Institute of Physics. [DOI: 10.1063/1.1849847]

GaInP/AlGaInP quantum well lasers emitting in the 620–690 nm wavelength range have a wide range of professional and consumer applications but are severely limited at high temperature or high power, particularly at the short wavelength end of the range, by the thermally activated leakage of electrons.^{1,2} One method to overcome such leakage current—the multiple quantum barrier (MQB)—was originally suggested by Iga³ and has been employed, with differing degrees of success, in laser structures fabricated from several different material systems including AlGaInP (e.g., Refs. 4 and 5). The MQB is incorporated into the *p*-side cladding region for the reflection of electrons in a manner analogous to the reflection of photons by a Bragg grating. It consists of thin (usually a quarter of the electron wavelength thick) layers of alternately large and small band gap material resulting in the formation of allowed and forbidden energy bands. The energetic position of these relative to the conduction band profile can be controlled by careful choice of well and barrier widths to enable a forbidden energy band to be aligned with the top of the cladding layer, which, along with an initial thick anti-tunneling layer, can lead to a virtual increase in the height of the electron potential barrier.

Although reductions in the threshold current of red-emitting lasers that include MQBs have been reported it is not always clear that the origin of the improvement is a reduction in the leakage current.⁶ In this work we compare the performance of a laser structure incorporating a MQB and a reference structure where the MQB is replaced with a layer of equivalent refractive index. We fully characterize both structures using the recently developed segmented contact method⁷ and show that the presence of a MQB does indeed improve performance by reducing thermally activated leakage current.

The two samples were grown by low pressure (150 Torr) MOCVD and both consisted of a 68-Å-wide single quantum well of $\text{Ga}_{0.41}\text{In}_{0.59}\text{P}$ emitting at 670 nm with a 900-Å-wide

layer of $(\text{Al}_{0.3}\text{Ga}_{0.7})\text{InP}$ on either side constituting the waveguide core. The MQB sample had an electron reflector in the *p*-cladding adjacent to the waveguide, which consisted of an initial anti-tunneling structure followed by six repeat cells of $(\text{Al}_{0.7}\text{Ga}_{0.3})\text{InP}$ barriers and $(\text{Al}_{0.3}\text{Ga}_{0.7})\text{InP}$ wells, both of which were 42 Å wide. This $3/4\lambda$ structure, incorporating indirect band gap material, was designed to produce an enhanced potential barrier to both gamma and X-band electrons. For the control sample an equivalent *p*-cladding layer with the average composition of the MQB was grown which consisted of a 945 Å layer of $(\text{Al}_{0.51}\text{Ga}_{0.49})\text{InP}$. Both samples also had an equivalent structure placed on the *n*-side so that the waveguide was symmetric. An additional 9000 Å of $(\text{Al}_{0.7}\text{Ga}_{0.3})\text{InP}$ cladding layer was grown outside of the core structure. The MQB structure is represented in schematic form in Fig. 1.

Threshold current measurements under pulsed operation (300 ns pulse, 1 kHz repetition rate) were made on both samples in the temperature range from 200 to 400 K for 50- μm -wide oxide isolated stripe devices with lengths of 320, 450, 600, and 750 μm . Results for the 320- and 450- μm -long devices are shown in Fig. 2. At low temperatures devices fabricated from both samples had the same threshold

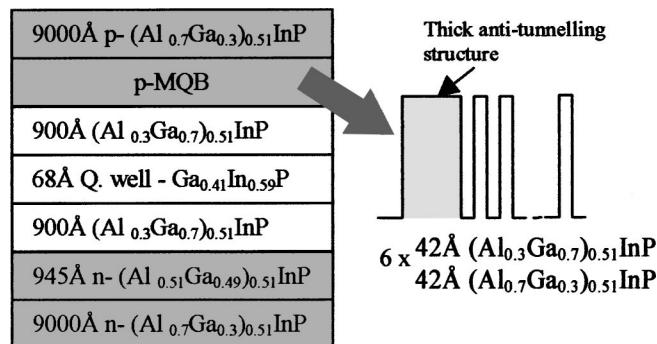


FIG. 1. Schematic diagram detailing the multilayers within the MQB laser structure.

^{a)}Electronic mail: smowtonpm@cf.ac.uk

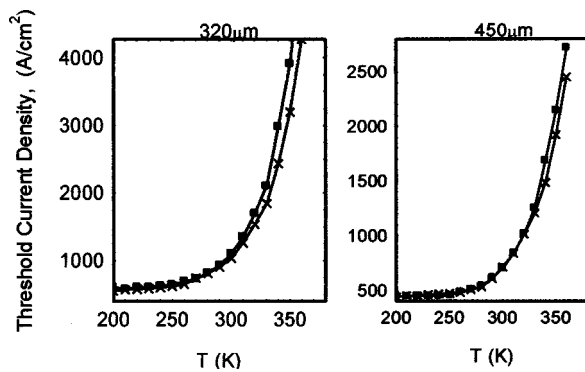


FIG. 2. Threshold current measurements, for the sample containing a MQB (crosses) and the control reference sample (squares), as a function of temperature.

current density to within the experimental error. However, at temperatures above 340 K, the sample with the MQB had a lower threshold current density than the control. Both samples operated as lasers up to approximately 380 K. The difference in threshold current density was measured to be 548 ± 38 A/cm² for the 320 μm devices and 202 ± 16 A/cm² for the 450 μm devices at 340 K increasing to 1735 ± 113 A/cm² and 1310 ± 85 A/cm², respectively, at 375 K. These differences were markedly smaller for longer devices. This behavior, where the threshold current is the same at low temperature but where a difference becomes apparent at higher temperature, is consistent with two structures having similar quantum wells but a different thermally activated leakage process. Furthermore, as the device length is reduced, the quasi-Fermi level separation necessary to achieve the threshold gain requirement increases, and the thermally activated leakage component of total current becomes more prevalent.⁸ The results obtained, where the largest reduction in threshold current density occurs for shorter devices at higher temperatures, indicates that the MQB is suppressing thermally activated leakage current.

Measurements of threshold current alone provide limited evidence of the beneficial effects of a MQB because they may be affected by variations in optical loss and well width. To eliminate any influence of these factors on our results we have studied the characteristics of samples fabricated from the two structures in more detail using the segmented contact method.⁹ We have determined the modal gain, internal optical mode loss, spontaneous emission, and quasi-Fermi level separation as a function of drive current density, over a range of temperatures to coincide with the previous measurements and, as before, used 300 ns pulses with a 1 kHz repetition rate. In particular, we focus on three temperatures, (a) 300 K, where *J*_{th} data indicated little or no difference between the two samples, (b) 340 K, where a small difference was observed for 450 μm devices, but a more significant difference was seen for the 320 μm devices and (c) 360 K, where the largest difference is observed for both lengths of device.

The internal optical mode loss, α_i , was found to be the same, within experimental uncertainty, for the two structures, being 5.0 ± 2 and 4.5 ± 2 cm⁻¹ for the control and MQB sample, respectively. The quasi-Fermi level separation at each drive current and temperature was determined from the transparency point on each gain spectrum⁷ and the radiative current density was derived from the true spontaneous emission spectra where the measurements in arbitrary units were

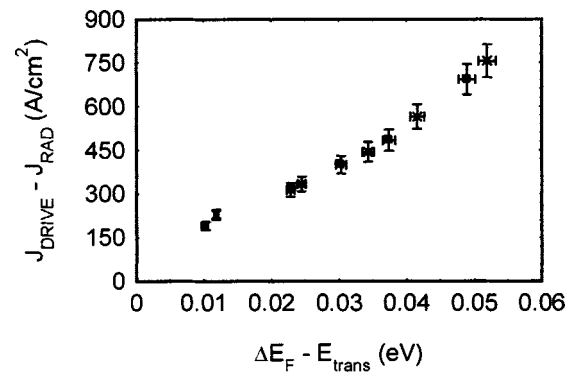


FIG. 3. Drive current density minus radiative current density as a function of quasi-Fermi level separation for the MQB (crosses) and control device (squares) at 300 K.

calibrated using the assumption that the inversion factor is unity at low energy.⁷ The total drive current density was calculated from the current used in the experiment and the device area.

The thermally activated leakage of electrons from the quantum well of a device is controlled by the energy of the electron quasi-Fermi level.⁹ For like structures one would expect the electron quasi-Fermi level to be similar for comparable values of the quasi-Fermi level separation. In this single pass, segmented contact experiment where stimulated emission is negligible,⁷ the difference between the total drive current density and the radiative current density is the nonradiative current density.

Nonradiative current density versus ($\Delta E_F - E_{trans}(T)$) is plotted at 300 K in Fig. 3 and at 340 K and 360 K in Fig. 4. The inclusion of the temperature-dependent transition energy, E_{trans} , obtained from photovoltage spectroscopy performed on the laser devices, removes any difference in ΔE_F caused by nonidentical active regions of the two structures.

At low temperatures the nonradiative current density is made up primarily of Shockley–Read–Hall recombination within the quantum well which might be expected to be comparable for the two structures and this is what is observed in Fig. 3 for data taken at 300 K and this is also the case for data taken at 250 K (not shown). At higher temperatures we expect thermally activated leakage to be a substantial factor in the nonradiative current density and if the MQB is suppress-

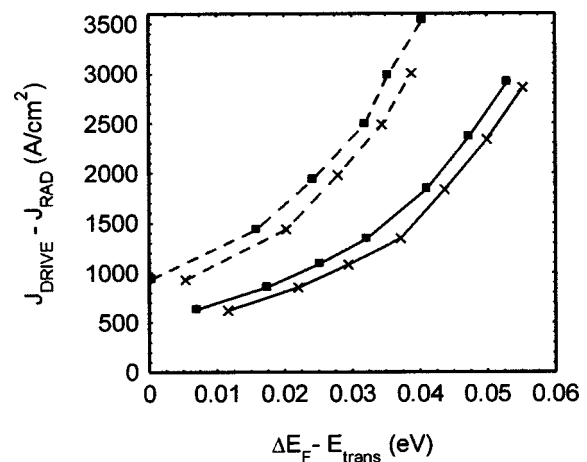


FIG. 4. Drive current density minus radiative current density as a function of quasi-Fermi level separation for the MQB (crosses) and control device (squares) at 340 K (solid) and 360 K (dashed).

ing the thermally activated leakage we would expect the total nonradiative current density to be different for the samples with and without the MQB and this is what is observed in Fig. 4 at temperatures of 340 and 360 K. To quantify this we consider the conditions necessary for operation of our 320- and 450- μm -long devices and relate the threshold current density data obtained from the laser devices with the nonradiative data obtained from the segmented contact measurements. We use the relation that at threshold the modal gain, G , minus the internal optical loss α_i , for a laser chip of length L is equal to the mirror loss α_m , i.e.,

$$G - \alpha_i = \alpha_m = \ln(1/0.29)/L, \quad (1)$$

where the reflectivity of the mirrors is taken to be 0.29. For the shorter devices of interest in this study, with lengths 320 and 450 μm , this corresponds to values of $(G - \alpha_i)$ of 38.7 and 27.5 cm^{-1} , respectively. These values can be equated into values of quasi-Fermi level separation using the Gain- $\Delta E_F - E_{\text{trans}}(T)$ characteristics obtained from the segmented contact data which can then be translated further into values of nonradiative current density. At 340 K, Fig. 4 shows that for both 450 and 320 μm device lengths of interest, corresponding to $(\Delta E_F - E_{\text{trans}}(T))$ of 31.6 ± 1.6 and 51 ± 1.6 meV, respectively, there is a reduction in nonradiative current density for the MQB sample of 168 ± 25 A/cm^2 for 450 μm devices and 449 ± 67 A/cm^2 for 320 μm devices. At 360 K, for a 450 μm device with $(\Delta E_F - E_{\text{trans}}(T))$ of 0.0357 eV, the nonradiative current density for the MQB and control samples is calculated to be 2639 ± 396 and 3025 ± 454 A/cm^2 , respectively, a decrease in nonradiative current of 13% for the sample containing the MQB. To obtain $G - \alpha_i$ of 38.7 cm^{-1} at 360 K using the large area segmented contact structures required drive currents in excess of those obtainable from our experimental apparatus. For this reason we were unable to make a comparison of 320 μm devices at this temperature. The difference in threshold current density for the devices with and without the MQB mea-

sured at 340 and 360 K are the same as the differences in nonradiative current density described earlier within the experimental uncertainty. This confirms that the reduction in threshold current density at high temperatures achieved by incorporating a MQB is due to a reduction in the thermally activated leakage current.

To summarize, we have investigated the performance of AlGaInP laser diodes with and without a MQB in the p -cladding. From threshold current density measurements we found, at higher temperatures, a reduction in threshold current density for the MQB sample compared to the control sample. Further analysis, using segmented contact data, indicated that this reduction in threshold current for a 450 μm laser device corresponded directly to a 13% reduction in nonradiative current density. This work has thus shown that by placing a MQB into the p -cladding layer of an AlGaInP 670 nm device, the amount of thermally activated electron leakage current density can be reduced.

The authors acknowledge the financial support of the UK EPSRC under Grant No. GR/S55767/01.

¹D. P. Bour, D. W. Treat, R. L. Thornton, R. S. Geels, and D. F. Welch, IEEE J. Quantum Electron. **29**, 1337 (1993).

²S. A. Wood, C. H. Molloy, P. M. Smowton, P. Blood, and C. C. Button, IEEE J. Quantum Electron. **36**, 742 (2000).

³K. Iga, H. Uenohara, and F. Koyama, Electron. Lett. **22**, 1008 (1986).

⁴K. Kishino, A. Kikuchi, Y. Kaneko, and I. Nomura, Appl. Phys. Lett. **58**, 1822 (1991).

⁵P. Raisch, R. Winterhoff, W. Wagner, M. Kessler, H. Schweizer, T. Riedl, R. Wirth, A. Hangleiter, and F. Scholz, Appl. Phys. Lett. **74**, 2158 (1999).

⁶A. P. Morrison, L. Considine, S. Walsh, N. Cordero, J. D. Lambkin, G. M. O'Connor, E. M. Daly, T. J. Glynn, and C. J. Van der Poel, IEEE J. Quantum Electron. **33**, 1338 (1997).

⁷P. Blood, G. M. Lewis, P. M. Smowton, H. D. Summers, J. D. Thomson, and J. Lutti, IEEE J. Sel. Top. Quantum Electron. **9**, 1275 (2003).

⁸P. M. Smowton, P. Blood, P. C. Mogensen, and D. P. Bour, Int. J. Optoelectron. **10**, 383 (1996).

⁹P. M. Smowton and P. Blood, IEEE J. Quantum Electron. **31**, 2159 (1995).